Interactions between Organized, Surface-Confined Monolayers and Vapor-Phase Probe Molecules. 11. Synthesis, Characterization, and Chemical Sensitivity of Self-Assembled Polydiacetylene/Calix[*n*]arene Bilayers

Daniel L. Dermody,[†] Richard M. Crooks,*[,†,‡] and Taisun Kim*[,§]

Contribution from the Department of Chemistry, Texas A&M University, College Station, Texas 77843-3255, and Department of Chemistry, Hallym University, Chuncheon, Kangwon-DO, South Korea

Received April 22, 1996. Revised Manuscript Received July 23, 1996[⊗]

Abstract: We report the synthesis and characterization of self-assembled polydiacetylene (PDA)/4-*tert*-butylcalix[*n*]arene (where $n = 4$ and 6, abbreviated as CA[4] and CA[6], respectively) bilayers on Au surfaces. The PDA/CA[*n*] bilayers act as chemically sensitive interfaces that are resistant to high thermal stresses and extreme electrochemical potentials, both of which may be encountered in technologically significant sensing applications. Moreover, these simply prepared bilayer materials are excellent protosystems for studying a range of important sensor-related issues. Here we discuss the linking chemistry that leads to calixarene immobilization and examine the role calixarenes play in vapor-phase sensing applications using surface acoustic wave (SAW) mass balances and Fourier transform infrared−external reflectance spectroscopy (FTIR-ERS). FTIR-ERS spectra indicate that CA[*n*] reacts with the acid chloride-terminated PDA self-assembled monolayers (SAMs) to form ester linkages. Using irreversible adsorption of vapor-phase *n*-butylamine onto the CA[*n*] bilayer-coated SAW devices as an indirect nanogravimetric probe of surface coverage, we calculate that CA[4] and CA[6] cover 58% and 61%, respectively, of the PDA surface. The irreversibly bound *n*-butylamine serves a secondary purpose by effectively filling voids between calixarenes, which hinders access to them by the vapor-phase molecules. Dosing the bilayer-coated SAW devices with VOCs after exposure to *n*-butylamine permits a better understanding of the role of the calixarene cavities relative to nonspecific adsorption at, for example, defect sites between CA[*n*] molecules. Additional control experiments involving PDA/CA[*n*] analogs, such as phenyl-terminated PDA, show that VOC adsorption is enhanced only on the CA[*n*] surfaces. This strongly suggests the presence of a specific interaction between the CA[*n*] cavities and VOCs rather than simple nonspecific adsorption.

Introduction

We report the synthesis and characterization of self-assembled polydiacetylene (PDA)/4-*tert*-butylcalix[*n*]arene (where $n = 4$ and 6, abbreviated as CA[4] and CA[6], respectively) bilayers on Au surfaces, Scheme 1. The PDA/CA[*n*] bilayers act as chemically sensitive interfaces that are resistant to high thermal stresses and extreme electrochemical potentials, both of which may be encountered in sensing applications. Moreover, these simply prepared bilayer materials are excellent protosystems for studying a range of important sensor-related issues. Here we discuss the linking chemistry that leads to calixarene immobilization and examine the role the calixarene cavities play in inducing selective binding of six volatile organic compounds (VOCs) using surface acoustic wave (SAW) mass balances and Fourier transform infrared−external reflectance spectroscopy (FTIR-ERS). We also discuss a new, general method for quantitatively determining calixarene surface coverages, and are therefore able to determine the relative surface concentrations of both hosts and guests.

CA[4] and CA[6] belong to a class of bucket-shaped molecules consisting of ($n = 4-11$) phenyl subunits.[1] In the cone conformation CA[4] and CA[6] have inner cavity diameters of 6.3 and 7.9 Å and outer upper-rim diameters of 13.6 and 18.0 Å, respectively.[2] The host−guest interactions associated with the hydrophobic CA[4] and CA[6] cavities are usually weak, since they involve principally van der Waals, induced-dipole, and $\pi-\pi$ stacking interactions. The strength and class of interactions between guest molecules and calixarenes can be tuned by varying the functional groups on the upper and lower calixarene rims, but these interactions are also generally fairly weak.[3]

The weak binding properties of calixarenes, coupled with the intrinsic size-selectivity of their cavities, make them (and related macrocycles)[4−6] excellent candidates for vapor-phase sensing of VOCs[7−13] and liquid-phase sensing of ions.[6,14,15] A recent

* To whom correspondence should be addressed.
† Texas A&M University.
‡ E-mail: crooks@chemvx.tamu.edu. Voice-mail: (409) 845-5629. Fax: (409) 845-1399.
§ Hallym University. E-mail: tskim@sun.hallym.ac.kr.
⊗ Abstract published in *Advance ACS Abstracts,* November 1, 1996.

(1) Gutsche, C. D. *Calixarenes*; The Royal Society of Chemistry: London, 1989.
(2) The edge-to edge internal cavity diameters and the upper outer-rim diameters of CA[4] and CA[6], in the cone conformation, were estimated from CPK models.
(3) Izatt, R. M.; Bradshaw, J. S.; Pawlak, K.; Bruening, R. L.; Tarbet, B. J. *Chem. Rev.* **1992**, *92*, 1261.
(4) Szejtli, J. *Cyclodextrins and their Inclusion Complexes*; Akademiai Kiado: Budapest, 1982.
(5) Saenger, W. *Angew. Chem., Int. Ed. Engl.* **1980**, *19*, 344.
(6) Rojas, M. T.; Köeniger, R.; Stoddart, J. F.; Kaifer, A. E. *J. Am. Chem. Soc.* **1995**, *117*, 336.
(7) Schierbaum, K. D.; Weiss, T.; Thoden van Velzen, E. U.; Engbersen, J. F. J.; Reinhoudt, D. N.; Göpel, W. *Science* **1994**, *265*, 1413.
(8) Schierbaum, K. D. *Sens. Actuators, B* **1994**, *18*, 71.
(9) Schierbaum, K.; Gerlach, A.; Göpel, W.; Muller, W.; Vögtle, F.; Dominik, A.; Roth, H. J. *Fresenius' J. Anal. Chem.* **1994**, *349*, 372.
(10) Dickert, F. L.; Bauer, P. A. *Adv. Mater.* **1991**, *3*, 436.

S0002-7863(96)01302-9 CCC: $12.00

Scheme 1

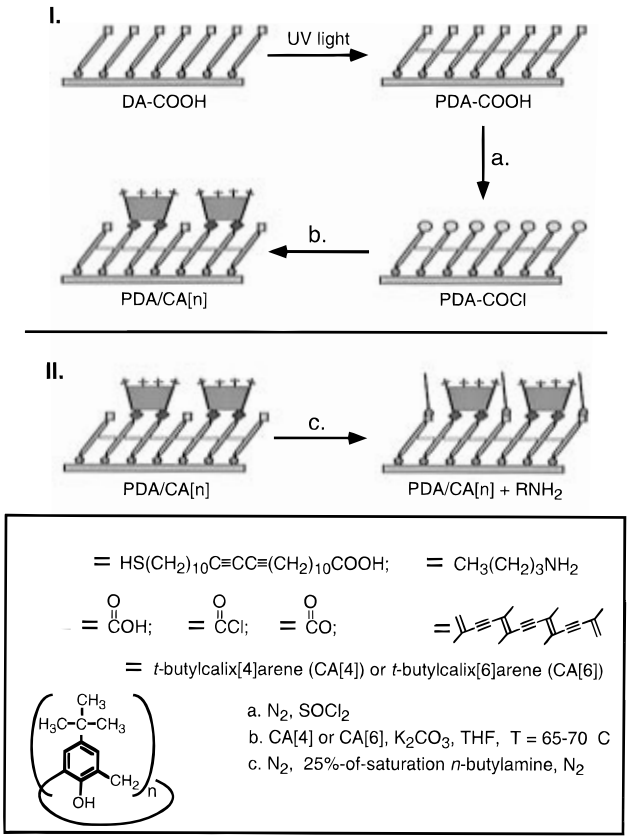

demonstration of VOC sensing by macrocycles was provided by Schierbaum et al., who described the structural and chemical properties of monolayers prepared from resorcin[4]arene macrocycles bound to Au surfaces through dialkyl sulfide tethers.[7] They provided evidence that the macrocycle headgroups act as molecular recognition sites that have high selectivity for tetrachloroethylene (C_2Cl_4). However, Grate and co-workers recently called this interpretation into question.[16] They argued that the VOCs interact primarily through nonspecific interactions with the calixarene surface rather than by specific host−guest interactions. Intercalation of VOCs into defects between calixarenes was thought to be a particular problematic channel for nonspecific adsorption.[16] The PDA/CA[4] and PDA/CA[6] bilayers described here provide a means for systematically distinguishing between specific and nonspecific VOC/calixarene film interactions. In this paper we compare the adsorption of six VOCs onto calixarene-modified bilayer surfaces and analogous control surfaces. The results demonstrate that the calixarene cavities dominate adsorption onto the calixarene surfaces through size, shape, and chemical selectivity that is absent on the control surfaces.

All previous approaches to covalent attachment of calixarene monolayers to transducers have involved synthetic manipulation of the calixarene lower rim.[7,8,10−14,16−19] This chemistry is generally cumbersome and time consuming. We avoid this problem here by using acid-terminated PDA self-assembled monolayers (SAMs) as adhesion layers for attaching commercially available calixarenes to Au surfaces. This greatly simplifies some of the synthetic aspects of macrocycle-based sensing and underscores the versatility of this general approach for preparing monolayers of related compounds such as cyclodextrins.[5,20,21] Synthetic flexibility is especially important for array-based sensing strategies, which relax selectivity requirements but necessitate simultaneous measurement of the interactions between analytes and many chemically distinct surfaces.[22] In addition, PDA SAMs contain few surface defects,[23] and therefore can effectively screen mass transport of VOCs to the underlying Au substrate,[23] they are more stable than all other organomercaptan SAMs,[24] and they can be patterned using standard photolithographic methods, which makes them amenable to microarray or combinatorial sensing approaches.[25]

Experimental Section

Chemicals. Thiophenol (Aldrich 99+%), phenol (Aldrich 99.9+%), 4-*tert*-butylphenol (Aldrich 99%), 4-*tert*-butylcalix[4]arene (Aldrich, 95%), 4-*tert*-butylcalix[6]arene (Aldrich, 95%), anhydrous tetrahydrofuran (THF) (Aldrich, 99.9%), potassium carbonate (K_2CO_3) (EM Science, 98.5%), acetone (EM Science, 99.5%), benzene (Aldrich, 99.5%), 1-butanol (Aldrich, 99.5%), *n*-butylamine (Aldrich, 99.4%), carbon tetrachloride (CCl_4) (Aldrich, 99.5%), *n*-heptane (Aldrich, 99+%), toluene (EM Science, 99.5%), trichloroethylene (TCE) (Aldrich, 99.5%), and 100% ethanol were used as received. Gaseous N_2 obtained from liquid N_2 boil-off was used for SAW device and FTIR-ERS experiments.

Substrate Preparation. Au-coated substrates were prepared by electron-beam deposition of 100 Å of Ti followed by 2000 Å of Au onto Si(100) wafers.[26] Au-coated SAW devices were prepared in the same manner on polished ST-cut quartz. Before each experiment all wafers and devices were cleaned in a low-energy Ar plasma cleaner at medium power for 1 min (Harrick Scientific Corp., New York, Model PDC-32G).

Part I of Scheme 1, illustrates the synthesis of the PDA/CA[*n*] bilayers (PDA/CA[*n*]). The synthesis and properties of HS-$(CH_2)_{10}C{\equiv}CC{\equiv}C(CH_2)_{10}X$ (X = COOH, DA-COOH, X = CH_3, DA-CH_3) have been discussed previously.[24,27,28] Monolayers were prepared by soaking a Au substrate in a 1 mM $CHCl_3$ solution of DA-COOH or DA-CH_3 for 4 h, removing the substrate from solution, rinsing with $CHCl_3$, and then drying under flowing N_2.[23] SAMs were polymerized by placing the DA-coated substrate in a sealed, N_2-purged polycarbonate chamber and exposing it to a UV light source (Oriel Model 6035) positioned about 1 cm from the substrate surface for 45 min. Following polymerization, the substrates were transferred to a glass reaction vessel and purged with N_2 for 10 min and then exposed to $SOCl_2$ vapor for 20 min. This procedure converts the carboxylic acid functional groups to the more reactive acid chloride (PDA-COCl).[27,29] CA[4] and CA-[6] are covalently bound to the PDA-COCl-modified Au substrate by

(11) Dickert, F. L.; Haunschild, A.; Reif, M.; Bulst, W. E. *Adv. Mater.* **1993**, *5*, 277.
(12) Nelli, P.; Dalcanale, E.; Faglia, G.; Sberveglieri, G.; Soncini, P. *Sens. Actuators, B* **1993**, *1993*, 302.
(13) Lai, C. S. I.; Moody, G. J.; Thomas, J. D. R.; Mulligan, D. C.; Stoddart, J. F.; Zarzycki, R. J. *J. Chem. Soc., Perkin Trans. 2* **1988**, 319.
(14) Forster, R. J.; Cadogan, A.; Diaz, M. T.; Diamond, D.; Harris, S. J.; McKervey, M. A. *Sens. Actuators, B* **1991**, *B4*, 325.
(15) Marsella, M. J.; Newland, R. J.; Carroll, P. J.; Swager, T. M. *J. Am. Chem. Soc.* **1995**, *117*, 9842.
(16) Grate, J. W.; Patrash, S. J.; Abraham, M. H.; Du, C. M. *Anal. Chem.* **1996**, *68*, 913.
(17) Adams, H.; Davis, F.; Sterling, C. J. M. *J. Chem. Soc., Chem. Commun.* **1994**, 2527.
(18) Davis, F.; Sterling, C. J. M. *J. Am. Chem. Soc.* **1995**, *117*, 10385.
(19) Thoden van Velzen, E. U.; Engbersen, J. F. J.; Reinhoudt, D. N. *J. Am. Chem. Soc.* **1994**, *116*, 3597.
(20) Lucklum, R.; Henning, B.; Hauptmann, P.; Schierbaum, K. D. *Sens. Actuators, A* **1991**, *A27*, 705.
(21) Ide, J.; Nakamoto, T.; Moriizumi, T. *Sens. Actuators, A* **1995**, *A49*, 73.
(22) Ricco, A. J. *Electrochem. Soc. Interface* **1994**, *3*, 38.
(23) Kim, T.; Chan, K.; Crooks, R. M. *Langmuir*, in press.
(24) Kim, T.; Ye, Q.; Sun, L.; Chan, K. C.; Crooks, R. M. *J. Am. Chem. Soc.*, in press.
(25) Chan, K. C.; Kim, T.; Schoer, J. K.; Crooks, R. M. *J. Am. Chem. Soc.* **1995**, *117*, 5875.
(26) Wells, M.; Dermody, D. L.; Yang, H. C.; Kim, T.; Crooks, R. M. *Langmuir* **1996**, *12*, 1989.
(27) Kim, T.; Crooks, R. M. *Tetrahedron Lett.* **1994**, *35*, 9501.
(28) Kim, T.; Crooks, R. M.; Ye, Q.; Sun, L. *J. Am. Chem. Soc.* **1995**, *117*, 3963.
(29) Deuvel, R. V.; Corn, R. M. *Anal. Chem.* **1992**, *4*, 337.

soaking it in a solution containing 300 mg each of CA[*n*] and K_2CO_3 dissolved in 10 mL of THF at $T = 65-70$ °C for 12 h. This yields the PDA/CA[*n*] bilayer linked through ester bonds between the acid chloride terminal groups of the PDA layer and the secondary hydroxyl groups of CA[4] and CA[6].[30] Prior to analysis, the bilayer-coated substrates were rinsed several times with acetone and deionized water (Milli-Q, Millipore, Bedford, MA) and then dried thoroughly under flowing N_2. The same procedure was used to prepare the PDA/phenyl (PDA/Ph) and PDA/4-*tert*-butylphenyl (PDA/*t*-Ph) bilayers.

The thiophenol (TP) monolayers were prepared by immersing a plasma-cleaned substrate in a 1 mM ethanolic solution of the TP for 16 h. Prior to analysis the monolayer-coated substrates were rinsed several times with ethanol and then dried under flowing N_2.

FTIR and SAW Measurements. FTIR-ERS measurements were made using a Digilab FTS-40 spectrometer equipped with a Harrick Scientific Seagull reflection accessory and a liquid-N_2-cooled MCT detector. All spectra were the sum of 256 individual scans using p-polarized light at an 84° angle of incidence with respect to the Au substrate.[31]

SAW device measurements were made at 25 ± 0.5 °C using two (98-MHz) ST-cut quartz oscillators housed in a custom-built flow system.[31] Modified SAW devices were dosed with vapor-phase probe molecules mixed down in N_2 at 25% of saturation (flow rate 0.5 L/min). The VOC vapor streams were prepared by bubbling a N_2 stream through the analyte and then mixing this 100%-of-saturation vapor with a second N_2 stream to achieve 25% of saturation. The saturation pressures of the 6 VOCs (mmHg at $T = 25$ °C), are calculated to be 95.2, 45.7, 115, 28.4, 6.2, and 69.1 for benzene, *n*-heptane, CCl_4, toluene, 1-butanol, and TCE, respectively.[32] The relative volatility of the six VOCs increases in the order butanol < toluene < *n*-heptane < TCE < benzene < CCl_4.

The change in SAW device frequency (Δf), due to the adsorption of vapor-phase molecules, is related to the mass loading per unit area (m_a) through the equation $\Delta f/f_o = -\kappa c_m f o m_a$. Here, f_o is the SAW resonance frequency (98 MHz), κ is the fraction of the distance between the centers of the transducers covered by the Au film (0.65), and c_m is the mass sensitivity coefficient of the device (1.33 $cm^2/(g\cdot MHz)$ for ST-cut quartz).[33,34] The frequency shift (Δf) of the SAW device should only be due to mass loading, rather than incorporating electrical and viscoelastic effects, since the PDA/CA[*n*] bilayers are thin, rigid, nonconducting films.[35]

The fractional *n*-butylamine coverage calculations assume a surface coverage of 0.78 nmol/cm^2 for hexagonal close-packed PDA adsorbing at the 3-fold hollow sites of a defect-free Au(111) surface. In calculating the surface coverage of *n*-butylamine, we assume a 1:1 reaction stoichiometry between it and the PDA SAMs. CA[*n*] surface coverages assume maximum coverages of 0.10 and 0.06 nmol/cm^2 for hexagonal close-packed CA[4] and CA[6] adsorbed on the PDA SAMs, respectfully. The theoretical maximum surface-concentration ratios of CA[4]:PDA and CA[6]:PDA are 1:7.8 and 1:13, respectively. All surface-coverage calculations incorporate an additional roughness factor of 1.2 ± 0.2.[26,31]

Results and Discussion

Figure 1 shows FTIR-ERS spectra of a PDA/CA[6] bilayer during each step of its preparation (Scheme 1). The most prominent peaks in the DA-COOH spectra are the asymmetric and symmetric methylene stretches (2928 and 2855 cm^{-1}, respectively) and the carboxylic acid C═O band at 1717 cm^{-1}.[31] The small feature at 1464 cm^{-1} probably arises from an α-CH_2 bending mode.[24] We attribute the small shoulder at 2960 cm^{-1}

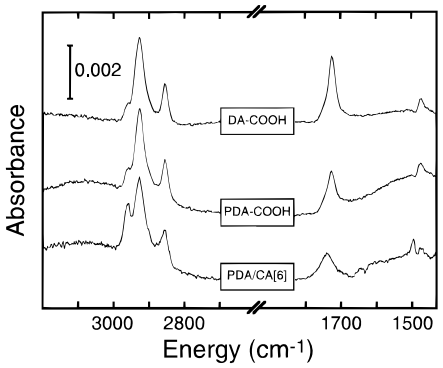

Figure 1. FTIR-ERS spectra of an acid-terminated diacetylene monolayer (DA-COOH), the same monolayer after polymerization (PDA-COOH), and the PDA-COOH SAM after covalent linking with 4-*tert*-butylcalix[6]arene (PDA/CA[6]).

to an asymmetric methyl stretch originating from adventitious hydrocarbons that adsorb on the high-energy acid surface. We have imaged such impurities on acid-terminated DA and PDA SAMs previously using scanning tunneling microscopy.[36] Polymerization (PDA-COOH) results in a decrease in the carbonyl band intensity, and the asymmetric and symmetric stretching bands shift to 2926 and 2854 cm^{-1}, which are all consistent with our previous findings.[28] Following activation of the SAM acid groups with $SOCl_2$ and reaction of the resulting acid chloride-terminated surface with CA[6], we observe the appearance of a strong asymmetric methyl stretch at 2960 cm^{-1}, which arises from the *tert*-butyl groups on the upper rim of the CA[6], and an aromatic stretching mode at 1487 cm^{-1} arising from the CA[6] phenyl rings.[37] The modes associated with phenyl rings are either very small or absent because of their orientation, substituent effects, and low surface concentrations. This result is consistent with control experiments discussed later. Importantly, the C═O band originally present at 1717 cm^{-1} shifts to 1736 cm^{-1} as a result of the new PDA/CA[6] ester linkage. This band is broad, which suggests the presence of both ester and unreacted acid carbonyl groups. We sonicated the substrates four times for 5 s each time in $CHCl_3$ to remove any physisorbed CA[6] from the surface but observed no change from the FTIR-ERS spectrum shown at the bottom of Figure 1.

To further confirm covalent attachment of CA[*n*] to the PDA-COOH surface, we performed two important control experiments. First, the synthetic procedure just described was carried out on an unreactive methyl-terminated PDA surface (PDA-CH_3).[24] Second, the same procedure was carried out on a PDA-COOH surface but without converting the acid groups to the acid chloride prior to CA[*n*] exposure. In both cases, and in contrast to the bilayers prepared on the PDA-COCl surfaces, the FTIR-ERS spectra of the SAMs obtained after processing and sonication were the same as those obtained from the initial monolayers.

To test the stability of the PDA/CA[*n*] bilayers, we subjected them to thermal and electrochemical desorption experiments. The bilayers withstood 5 min thermal stresses of $T = 200$ °C in flowing Ar, as well as extreme electrochemical potentials, (32 scans between −1.4 and −0.5 V (vs a Ag/AgCl reference electrode)), without appreciable loss of PDA/CA[*n*] as measured by FTIR-ERS.[24] Similar conditions result in complete desorption of simple *n*-alkanethiol SAMs.[24,38]

(30) March, J. *Advanced Organic Chemistry*; Wiley-Interscience: New York, 1987.
(31) Yang, H. C.; Dermody, D. L.; Xu, C.; Ricco, A. J.; Crooks, R. M. *Langmuir* **1996**, *12*, 726.
(32) Dean, J. A. *Lange's Handbook of Chemistry*, 12th ed.; McGraw-Hill: New York, 1979.
(33) Thomas, R. C.; Sun, L.; Crooks, R. M.; Ricco, A. J. *Langmuir* **1991**, *7*, 620.
(34) Wohltjen, H. *Sens. Actuators* **1984**, *5*, 307.
(35) Martin, J. S.; Frye, G. C.; Senturia, S. D. *Anal. Chem.* **1994**, *66*, 2201.
(36) Schoer, J. K.; Zamborini, F. P.; Crooks, R. M. Unpublished results.
(37) Colthup, N. B.; Daly, L. H.; Wiberly, S. E. *Introduction to Infrared and Raman Spectroscopy*, 3rd ed.; Academic Press, Inc.: San Diego, 1990.
(38) Widrig, C. A.; Chung, C.; Porter, M. D. *J. Electroanal. Chem.* **1991**, *310*, 335.

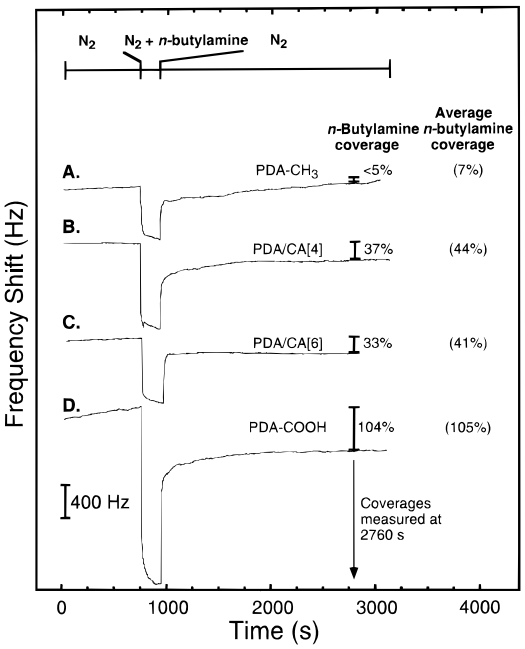

Figure 2. Representative real-time surface acoustic wave device frequency responses obtained for the SAMs (A) PDA-CH_3, (B) PDA/CA[4], (C) PDA/CA[6], and (D) PDA-COOH before, during, and after exposure to 25%-of-saturation *n*-butylamine vapor mixed down in dry N_2. The percentage of the surface that reacts with *n*-butylamine in this particular experiment is indicated on the right side of the figure. The average percentage, obtained from duplicate experiments, is shown in parentheses. Coverages are corrected for a surface roughness factor of 1.2 ± 0.2.

Part II of Scheme 1 illustrates a novel nanogravimetric method for determining the extent of CA[*n*] surface coverage on the PDA SAM.[6] The method is generally applicable to many other reactive surfaces. We have previously shown that vapor-phase primary amines, such as *n*-butylamine, irreversibly bind to acid-terminated SAMs but that they readily desorb from low-energy surfaces such as the PDA-CH_3 or hydrophobic cavities of calixarenes.[31] The *n*-butylamine interacts weakly and reversibly with the calix[*n*]arene cavity, via hydrogen-bonding and van der Waals interactions, and irreversibly with the remaining PDA-COOH headgroups via proton transfer. By measuring the difference in *n*-butylamine mass loading on the PDA-COOH and PDA/CA[*n*] surfaces, the fractional surface coverage of CA-[*n*] on the PDA surface can be approximated.[26,34,35] The results of this experiment are shown in Figure 2.

Figure 2A is the real-time SAW device response resulting from exposure of a PDA-CH_3 surface to *n*-butylamine vapor. We allowed the SAW device to stabilize in a pure N_2 purge for 750 s and then switched to a 25%-of-saturation *n*-butylamine vapor for an additional 210 s. When the experiment had run for 960 s, the SAW device was again purged with pure N_2. This same procedure was followed for the other three experiments illustrated in Figure 2. Upon exposure to *n*-butylamine, we observe a rather large mass increase, which arises primarily from *n*-butylamine weakly bound to the low-energy methyl surface. After purging with N_2 for 1800 s, all of this material desorbs except for an amount corresponding to <5% of a monolayer. We performed experiments like this twice, and obtained an average surface coverage of 7%. This level of adsorption may result from tenacious binding of the amine to the unmetalated part of the quartz SAW device.

Parts B and C of Figure 2 show the results of similar experiments performed on PDA/CA[4] and PDA/CA[6] surfaces, respectively. For these particular experiments, the

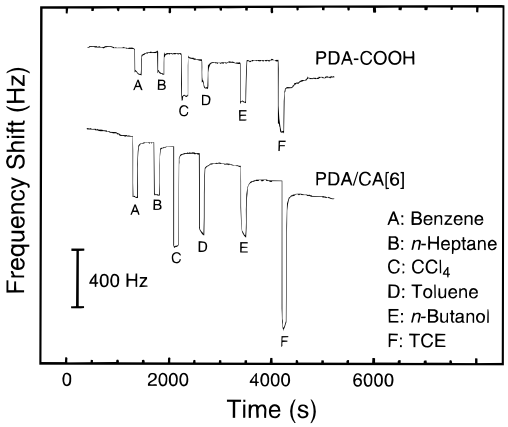

Figure 3. Frequency responses of PDA-COOH- and PDA/CA[6]-coated SAW devices exposed to (A) benzene, (B) *n*-heptane, (C) CCl_4, (D) toluene, (E) 1-butanol, and (F) TCE at 25% of saturation mixed down in dry N_2.

n-butylamine surface coverages on the PDA/CA[4] and PDA/CA[6] bilayers are 37% and 33%, respectively, whereas the average *n*-butylamine coverages are 44% and 41%, respectively. Dosing the unreacted PDA-COOH surface with *n*-butylamine (Figure 2D) yields single-experiment and average *n*-butylamine surface coverages of 104% and 105%, respectively. The average surface coverages were obtained from the results of two experiments performed on independently prepared SAW devices, and the error margin was less than ±10% of a monolayer in all cases. Similar experiments conducted on the PDA/phenyl (PDA/Ph) and PDA/4-*tert*-butylphenyl (PDA/*t*-Ph) bilayers result in an average *n*-butylamine surface coverage of 5% and 4%, respectively.

We can use the preceding results to estimate the fractional coverage of CA[4] and CA[6] on the bilayer surfaces by subtracting the average *n*-butylamine coverage on the PDA/CA[4] and PDA/CA[6] bilayers from the average *n*-butylamine surface coverage on the PDA-COOH surface and dividing the difference by the PDA-COOH surface coverage. We calculate that CA[4] and CA[6] cover 58% and 61%, respectively, of the PDA-COOH surface. These values correspond to surface concentrations of 0.06 and 0.04 nmol/cm^2 for CA[4] and CA-[6], respectively. This somewhat low surface coverage, which reflects the poor packing ability of the calixarenes, is not surprising given their conical shape, the sterically confining *tert*-butyl groups on the upper rim, and their inability to surface diffuse to form close-packed monolayers. Moreover, these results are comparable to the 64−75% coverages, based upon electrochemical reductive desorption of thiolated species, found by Kaifer et al. for thiolated β-cyclodextrin directly bound to Au.[6]

Figure 3 shows unprocessed, real-time SAW device responses resulting from the reversible adsorption of 25%-of-saturation benzene, *n*-heptane, CCl_4, toluene, 1-butanol, and TCE vapors on PDA-COOH and PDA/CA[6] surfaces. Each of these experiments was performed twice, with the error margin being less than ±10% of a monolayer in all cases. With the exception of TCE, adsorption and desorption of the volatile organic compounds (VOCs) on both PDA-COOH and PDA/CA[6] surfaces are both rapid (∼5 s) and reversible. We speculate that the slow desorption of TCE (up to 3 h on the PDA-COOH surface) may result from intercalation of a small percentage of the TCE into packing-defect voids within the PDA film. At least in the case of toluene, the adsorption isotherm connecting the vapor and surface concentrations is linear over the range 0−25% of saturation. Duplicate VOC dosing experiments were performed using the same SAW devices, approximately 1 month

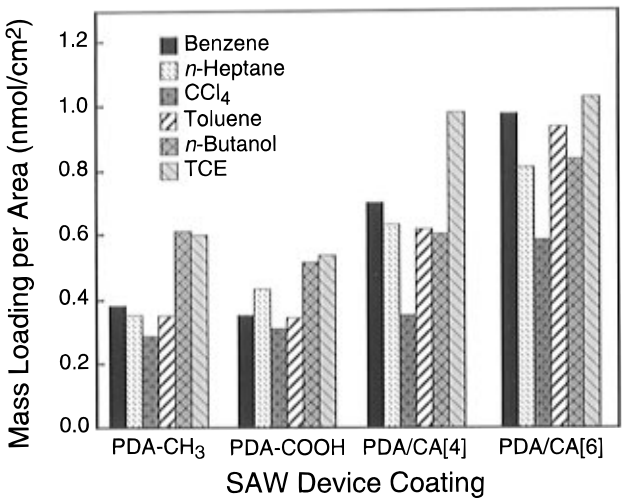

Figure 4. Comparison of the average mass loading per area for PDA-CH_3-, PDA-COOH-, PDA/CA[4]-, and PDA/CA[6]-coated SAW devices exposed to six volatile organic compounds (VOCs) present at 25% of saturation mixed down in dry N_2.

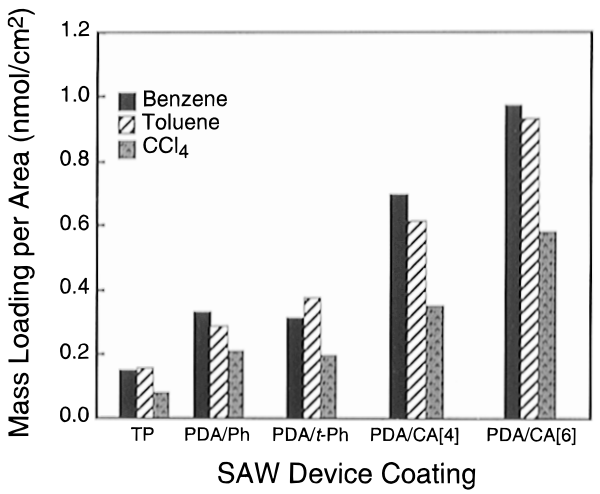

Figure 5. Comparison of the average mass loading per area for TP-, PDA/Ph-, PDA/*t*-Ph-, PDA/CA[4]-, and PDA/CA[6]-coated SAW devices exposed to benzene, toluene, and CCl_4 present at 25% of saturation mixed down in dry N_2.

after those shown in Figure 3, to verify the stability of the SAM surfaces. In each case, the results were within 10% of a monolayer of their original values. Taken together, these experiments demonstrate that the interactions between VOCs and CA[*n*] surfaces are generally reversible and reproducible, and that a linear correspondence connects the bulk and surface concentrations. Moreover, the bilayers themselves are stable for long periods of time. These characteristics are highly desirable in sensor design.

Figure 4 shows a summary of the average mass-loading data obtained from dosing the PDA-COOH and PDA-CH_3 monolayer- and PDA/CA[4] and PDA/CA[6] bilayer-coated SAW devices with six VOCs. The bilayer-coated devices generally give higher mass-loading responses relative to the PDA-coated devices. We anticipated this result because of the enhanced binding between the calixarene cavities and the VOCs compared to their nonspecific interactions with the PDA-CH_3 and PDA-COOH surfaces.

To better understand the adsorptive behavior of the calixarene cavities, relative to nonspecific adsorption at, for example, defect sites between CA[*n*] molecules, we dosed the same bilayer-coated SAW devices used to obtain the data shown in Figures 3 and 4 first with *n*-butylamine, in an effort to passivate the voids between calixarenes, and then again with the six VOCs.[6] After irreversible adsorption of a quantity of *n*-butylamine consistent with the data shown in Figure 2B,C, the frequency responses of the CA[4]- and CA[6]-coated devices were within 5% of a monolayer of their original values for all six VOCs. This strongly suggests that enhanced VOC adsorption at the calixarene-modified surface results from the cavities rather than interstitial voids. As a control experiment we also dosed the PDA-CH_3- and PDA-COOH-coated SAW devices with 25% of saturation benzene after dosing them with *n*-butylamine and found the frequency responses due to benzene adsorption were also within 5% of a monolayer of the original values.

Figure 5 shows a summary of the average mass-loading data obtained from dosing thiophenol (TP)-, phenyl-terminated PDA (PDA/Ph)-, 4-*tert*-butylphenyl-terminated PDA (PDA/*t*-Ph)-, PDA/CA[4]-, and PDA/CA[6]-coated SAW devices with 25%-of-saturation benzene, toluene, and CCl_4. The TP, PDA/Ph, and PDA/*t*-Ph control surfaces were chosen because of their structural similarity to the PDA/CA[*n*] bilayers, but note the absence of a distinct cavity on the control surfaces. TP is bound to the Au substrate directly through thiol−Au bonds while Ph and *t*-Ph are linked to the PDA layer through ester linkages in the same manner as CA[*n*].

We dosed the TP, PDA/Ph, and PDA/*t*-Ph surfaces to determine whether VOC adsorption is enhanced at the CA[*n*] surfaces on the basis of specific interactions with discrete CA-[*n*] macrocycles or whether nonspecific interactions, promoted by the calixarene *tert*-butylphenyl groups, dominate adsorption. Referring to Figure 5, the magnitude of VOC adsorption is much smaller, typically less than 50%, for the TP, PDA/Ph, and PDA/*t*-Ph surfaces compared to the PDA/CA[*n*] bilayers. We would expect that if the adsorption enhancement observed for the CA-[*n*] surfaces results primarily from nonspecific interactions between the VOCs and the functional groups on the CA[*n*] upper rim, then a similar extent of VOC adsorption would occur at the TP, PDA/Ph, and PDA/*t*-Ph surfaces. These control experiments clearly underscore the necessity of the macrocyclic structure of the CA[*n*] surfaces for VOC adsorption enhancement.

On the basis of the data in Figure 5, we conclude that the calixarenes retain their cone conformations when confined to the PDA surface. Evidence for this comes from the enhanced adsorption noted for benzene and toluene on the CA[*n*] surfaces compared to TP, PDA/Ph, and PDA/*t*-Ph surfaces. The CA[4] and CA[6] cavities have interior diameters of 6.3 and 7.9 Å, respectively.[2] The benzene and toluene molecules have estimated molecular diameters, across the 2,6-hydrogens, of 6.3 Å (CPK models), and their flat, discus-like shapes are conducive to inclusion within the CA[*n*] cavities. Thus, we conclude that enhanced selectivity for benzene and toluene results from a favorable specific interaction between the hydrophobic cavities of the two calixarenes and the two aromatic compounds, which is only possible if the calixarenes retain their cone conformations.

Additional evidence for retention of the calixarene shape on the surface comes from a comparison of the CCl_4 data (Figure 5). The PDA/CA[6] bilayer is more receptive to the CCl_4 probe than the PDA/CA[4], PDA/*t*-Ph, PDA/Ph, and TP surfaces. We interpret this result in terms of size and shape selectivity, which would not be possible if the calixarenes unfolded on the PDA surface. Unlike benzene or toluene, CCl_4 has spherical symmetry and is too large (approximately 6.4 Å in diameter based on CPK models) to fit entirely within the CA[4] cavity, but it is sufficiently small to be accommodated by CA[6]. That the calixarenes retain their cone conformations on the PDA surface

is not surprising, since there is steric crowding on the lower rims, and because the calixarene conformations are locked in on the surface by covalent bonds to the PDA SAM.[6]

There is one final very interesting issue raised by the data in Figure 5. As discussed earlier, CA[4] and CA[6] have estimated surface coverages of 0.06 and 0.04 nmol/cm^2, respectively. Dosing the CA[4] and CA[6] surfaces with 25%-of-saturation benzene yields mass loadings of 0.70 and 0.97 nmol/cm^2, respectively. Since a 1:1 host:guest stoichiometry would yield maximum benzene coverages equal to the CA[4] and CA[6] surface concentrations, we conclude that the calixarenes act as templates that nucleate benzene into clusters that average 10−20 molecules each and permit it (as well as some of the other probe molecules) to adopt surface conformations that are to some degree solid-like. That is, whatever phase the surface-confined benzene is in, it has a lower vapor pressure than liquid benzene or else it would immediately desorb from the surface. Importantly, on the three non-calixarene surfaces shown in Figure 5, the surface concentration of benzene does not exceed half of the maximum single-monolayer coverage (roughly the same as the PDA monolayer: 0.94 nmol/cm^2), which provides an important control that strongly suggests the fully reproducible data for CA[4] and CA[6] surfaces are correct. Finally, we note that we have observed an identical templating effect for a different monolayer system, and together with these results we suggest that this phenomenon might be quite general.[39]

Summary and Conclusion

We have discussed the synthesis, characterization, and sensor-related chemistry of Au-bound polydiacetylene/4-*tert*-butylcalix[*n*]arene bilayers. For example, we employed specific vapor-phase probe molecules and SAW devices to estimate the calixarene surface coverage. We also differentiated the roles of the calixarene cavities, the voids between calixarenes, and the voids between molecules comprising the PDA adhesion layer toward vapor-phase probe molecules. FTIR-ERS and SAW experiments show the potential of PDA/CA[*n*] bilayers as rugged, sensitive coatings for vapor-phase chemical sensing applications. Moreover, and perhaps most significantly, the attachment chemistry we describe is highly versatile and should be useful for surface immobilization of other receptor monolayers.

We are currently improving our synthetic method to optimize the packing density of the CA[*n*] molecules on the PDA surface. We are also working toward incorporation of calixarenes having different functional groups on the upper rims and a variety of tailored cyclodextrin species into array-based sensing strategies. These experiments will provide us with a better understanding of how molecularly inclusive thin films interact with vapor- and liquid-phase analytes.

Acknowledgment. R.M.C. and D.L.D. gratefully acknowledge financial support from the National Science Foundation (Grant CHE-9313441). T.K. acknowledges financial support from the Hallym Academy of Sciences, Hallym University. We have benefited greatly from discussions with Dr. Antonio J. Ricco (Sandia National Laboratories). We also appreciate the suggestion of obtaining SAW device data from the TP, PDA/Ph, and PDA/*t*-Ph surfaces made by Diane K. Smith (San Diego State University).

JA961302X

(39) Thomas, R. C.; Yang, H. C.; DiRubio, C. R.; Ricco, A. J.; Crooks, R. M. *Langmuir* **1996**, *12*, 2239.